IEEE Photonics Journal
An IEEE Photonics Society Publication

Open Access

# Broadly Tunable Self-injection Locked InAs/InP Quantum-dash Laser Based Fiber/FSO/Hybrid Fiber-FSO Communication at 1610 nm

Volume 10, Number 2, April 2018

M. A. Shemis
E. Alkhazraji
A. M. Ragheb
M. T. A. Khan, *Student Member, IEEE*
M. Esmail, *Member, IEEE*
H. Fathallah, *Senior Member, IEEE*
S. A. Alshebeili
M. Z. M. Khan, *Senior Member, IEEE*

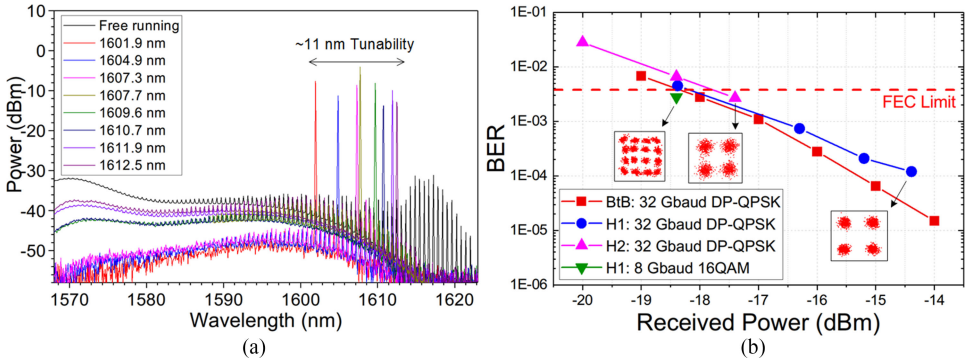


DOI: 10.1109/JPHOT.2018.2809566

# Broadly Tunable Self-injection Locked InAs/InP Quantum-dash Laser Based Fiber/FSO/Hybrid Fiber-FSO Communication at 1610 nm

**M. A. Shemis,[1] E. Alkhazraji,[1,2] A. M. Ragheb,[3] M. T. A. Khan,[1] *Student Member, IEEE*, M. Esmail,[3] *Member, IEEE*, H. Fathallah,[4] *Senior Member, IEEE*, S. A. Alshebeili,[3,5] and M. Z. M. Khan,[1] *Senior Member, IEEE***

[1]Optoelectronics Research Laboratory, Electrical Engineering Department, King Fahd University of Petroleum and Minerals, Dhahran 31261, Saudi Arabia
[2]Department of Electrical and Electronics Engineering Technology, Jubail Industrial College, Jubail 31961, Saudi Arabia
[3]KACST-TIC in Radio Frequency and Photonics for the e-Society (RFTONICS), Riyadh 11421, Saudi Arabia
[4]Laboratory of Physics of Materials-Structures and Properties, Computer Department, Faculty of Sciences of Bizerte, University of Carthage, Tunis 1054, Tunisia
[5]Electrical Engineering Department, King Saud University, Riyadh 11421, Saudi Arabia

*DOI:10.1109/JPHOT.2018.2809566*


Manuscript received February 16, 2018; accepted February 22, 2018. Date of publication February 27, 2018; date of current version March 30, 2018. This work was supported in part by the King Fahd University of Petroleum and Minerals through Grant KAUST004, in part by the King Saud University through research group RG-1438-092, and in part by KACST-TIC in SSL via Grant EE2381. *(M. A. Shemis and E. Alkhazraji contributed equally to this work.)* Corresponding author: M. Z. M. Khan (e-mail: zahedmk@kfupm.edu.sa).

**Abstract:** We report a self-injection-locked InAs/InP quantum-dash tunable laser with ∼11 nm (∼1602–1613 nm) tuning window for next generation multiuser ultrahigh capacity fiber/free-space optics (FSO)/hybrid fiber-FSO-based optical networks. A tunability of >18 independently locked subcarriers with ∼28 dB side mode suppression ratio (SMSR) and stable (±0.1 dBm) mode power is exhibited, and an estimated small injection ratio of ∼–22 dBm is found to sustain locking and SMSR. Error free transmission of 100 and 128 Gb/s externally modulated dual-polarization quadrature phase shift keying (DP-QPSK) signals over 20 km single mode fiber (SMF) and 16 m indoor FSO links are demonstrated across 8 and 4 individual subcarriers, respectively, thus covering the entire tuning range. Moreover, up to 168 (192) Gb/s successful transmission over 10 km SMF (BTB) and 176 Gb/s over 16 m FSO link is achieved on a ∼1610 nm subcarrier. Finally, a 128 Gb/s DP-QPSK transmission over 11 km SMF–8 m FSO–11 km SMF hybrid system is accomplished, thus paving the potential deployment of this single-chip, cost-effective, and energy efficient tunable light source in terabits/s next-generation passive optical networks.

**Index Terms:** Coherent communication, quantum-dash laser diode, self-injection locking, tunable laser sources, optical access networks, hybrid fiber-FSO system.

## 1. Introduction

Currently, the need for high bandwidth optical communication networks is intensifying owing to the sharp increase in both the number of end-users and their demand for high speed mobile

TABLE 1

Tunability of Various C- and L-Band Sources Employed in Single Channel Fiber/FSO Transmission, and Comparison of Various Hybrid Fiber-FSO Systems Reported in Literature, Sorted Respectively, With Increasing Data Rate

| Source | Data Rate (Gb/s) | Tunability (nm) | Wavelength (nm) | Modulation Scheme | Channel | Assisting Scheme | Ref. |
|---|---|---|---|---|---|---|---|
| RSOA | 1.25 (D) | ~6 (TBPF) | C-band (~1554-1560) | OOK | 21 km SMF | SIL | [10] |
| FP-LD | 2.5 (D) | ~20 (TBPF) | C-band (~1536-1556) | OOK | 85 km SMF | SIL | [11] |
| WFP-LD | 10 (D) | ~34 (C) | C-band (~1528-1562) | 16QAM-OFDM | 60 km SMF | EIL | [7] |
| FP-LD | 10 (D) | ~10 (FBG) | C-band (~1530-1540) | OOK | 20 km SMF | SIL | [12] |
| WFP-LD | 20 (D) | ~13 (C) | nL band (~1575-1588) | 16QAM-OFDM | 25 km SMF | EIL | [8] |
| BLS | 40 (E) | - | C-band (~1540) | OOK | 150 m I-FSO | OEO | [18] |
| QD-LD | 100 (E)<br>100 (E) | ~23 (C) | fL-band (~1611-1634) | DP-QPSK | 10 km SMF<br>4 m I-FSO | EIL | [9]<br>[21] |
| QD-LD | 128 (E) | ~6 (TBPF) | mL-band (~1601-1607) | DP-QPSK | 5 m I-FSO | SIL | [22] |
| QD-LD | 128 (E) | MWS* (18 modes) | mL-band (~1600-1610) | DP-QPSK | 20 km SMF | SIL | [16] |
| QD-LD | 128 (E) | - | mL-band (~1607) | DP-QPSK | 10 m I-FSO | SIL | [17] |
| QD-LD | 168 (E)<br>176 (E) | ~11 (TBPF) | mL-band (~1602-1613) | DP-QPSK | 10 km SMF<br>16 m I-FSO | SIL | This work |
| QD-LD | 200 (E) | MWS* (60 modes) | C-band (~1538-1545) | PM-QPSK | 75 km SMF | ML | [15] |
| DFB | 320 (E) | - | C-band (~1550) | DP -16QAM | 100 m O-FSO | - | [18] |
| ECL | 5 (E) | - | C-band (~1550) | DP-QPSK | 100km SMF-54m O-FSO | - | [22] |
| DFB | 10 (E) | - | C-band (~1550) | 16QAM | 40km SMF-6m I-FSO | - | [23] |
| Laser Array | 10 (E) | - | C-band (~1550) | NRZ | 40km SMF-10m O-FSO-40km SMF | - | [20] |
| QD-LD | 32 (E) | ~11 (TBPF) | mL-band (~1608) | 16QAM | 11Km SMF-8m I- FSO | SIL | This work |
| DFB | 90 (E) | - | C-band (~1550) | 32QAM | 11km SMF-100m O-FSO | - | [4] |
| Laser Array | 100 (E) | - | C-band (~1550) | DP-QPSK | 40km SMF-80m O-FSO | - | [5] |
| QD-LD | 128 (E) | ~11 (TBPF) | mL-band (~1608) | DP-QPSK | 11km SMF-8m I- FSO-11km SMF | SIL | This work |

"C" correspond to conventional tuning via external tunable laser source/broadband light source
"D" and "E" correspond to direct- and external-modulation, respectively, "OEO" correspond to optoelectronic oscillator, and "nL", "mL" and "fL" correspond to near-, mid- and far-L-band, O/I-FSO: Outdoor/Indoor free space optical communication
*multiwavelength/frequency comb source with corresponding sub-carriers

and internet connectivity. It is estimated that there will be more than 4.6 billion internet users with 27.1 billion global IP networked devices by the end of 2021 [1]. In this respect, wavelength division multiplexed (WDM) based passive optical networks (WDM-PONs) providing simultaneous connectivity to multiple remote locations, have been acknowledged as a potential low-cost scheme for 10G, 100G and 400G NG-PONs that are being developed to provide higher bandwidth solutions with better privacy and scalability [2]. In literature, generally two research routes are being explored to mitigate the future requirements; first addressing transmitter/receiver requirements of being energy efficient, mass producible and deployable for cost-effective capital (CAPEX) and operation (OPEX) expenditure, for WDM-PONs, thus relying on the existing network infrastructure [3]. Other route is examining alternate network architectures such as free space optical communication (FSO), which benefits from the shared optical domain with the fiber infrastructure, and hybrid fiber-FSO systems. In fact, FSO and hybrid fiber-FSO architectures are already garnering attention for both indoor and outdoor networks, and as a supplementary or supporting solution, or as a pure system backhaul replacement [4]–[6]. A brief review of recent achievements in fiber, FSO and hybrid fiber-FSO systems, is summarized in Table 1.

Several WDM-PON architectures employing a variety of light sources have been reported in the literature, with injection-locked schemes being highly attractive owing to their "colorless" feature, thereby enabling dynamic wavelength allocation to the subscribers [3]. External injection-locking (EIL) [7]–[9] using a tunable laser source (TLS) or a broadband light source (BLS) as master source enabled successful transmission of 60 km–10 Gb/s and 10 km–100 Gb/s data rates over SMF, by employing weak resonant-cavity Fabry-Perot laser diode (WFP-LD) and quantum-dash laser diodes (QD-LD), respectively [7], [9]. The corresponding source Fabry-Perot (FP) mode wavelength tunability was ∼34 nm and ∼23 nm in C- and L-bands, and achieved by conventional scheme (*i.e.*, by an external seeding light source). On another front, self-injection locking (SIL) in PONs was also investigated employing C-band self-seeded RSOA [10] and Fabry Perot laser diodes (FP-LD) [11], [12] with up to 10 Gb/s OOK transmission over 20 km SMF. While the former source exhibited locked FP mode tunability of ∼6 nm by utilizing a tunable band pass filter (TBPF) [10], the latter source exploited different fiber Bragg gratings (FBG) [12] to demonstrate ∼20 nm tunability. Moreover, sophisticated architectures based on modulation averaging reflector [13] and Faraday's rotating mirror [14] have also been utilized with 1.25 Gb/s-60 km and 1.25 Gb/s–25 km transmission over C-bands, respectively. QD-LD has also been employed as a frequency comb source in WDM-PON, exhibiting simultaneous generation of ∼60 and ∼16 FP modes via mode locking (ML) [15] and SIL [16] assisting techniques and emitting in C- and L-bands, respectively. Besides, a comprehensive comparison of EIL and SIL on QD-LD was also investigated in [17].

On the other hand, in literature, the viability of FSO has been principally reported with BLS [18], FP-LD and DFB laser diodes [19], targeting potential outdoor applications such as; transitional and temporary network connection, network access in isolated premises, etc. [20], and indoor deployment for data centers and high-performance computing [21]. Very recently, the integration of FSO with fiber technology (hybrid fiber-FSO) has being recognized as a promising network infrastructure for first/last mile optical access networks with various demonstrations, as summarized in Table 1, and mostly concentrating in C-band [20]–[23]. In summary, date rates up to 100 Gb/s, hybrid links comprising of 100 km fiber length or 100 m FSO channels, have been reported. Besides, real-time [22] and cable television (CATV) [6] transmission of signals are also demonstrated on this hybrid network. Alternatively, convergence of injection-locked WDM system with this network infrastructure is a promising NG-PON, thus providing flexibility and scalability, and low CAPEX and OPEX, compared to fiber-counterpart. Besides, penetration of this technology for indoor applications would enable realization of adaptive mega data centers for rack-to-rack, intra-rack, and card-to-card communication, enabling easy upgradability [21]. Hence, with this standpoint, we recently demonstrated 4 m–100 Gb/s indoor FSO link employing a ∼23 nm tunable external injection-locked QD-LD [24], and very recently 5 m–128 Gb/s via ∼6 nm tunable self-injection locked QD-LD [25] and 10 m–128 Gb/s [17] FSO links, in mid L-band region.

In this work, we aim to investigate the potential of employing this new class of self-injection locked tunable QD-LD in existing fiber technology, and alternate FSO and hybrid fiber-FSO systems. This is carried out by firstly reporting an extended tuning window of ∼11 nm from the QD-LD, thus covering ∼18 independently locked subcarriers with >28 dB SMSR. Moreover, we comprehensively investigated the performance of the tunable laser from short-term stability analysis of mode power, SMSR and wavelength of various single locked modes across the tuning range, and injection ratio requirements perspective, to shed light onto the device physics. Thereafter, we report separate 100 and 128 Gb/s DP-QPSK error free transmission over 20 km SMF and 16 m indoor FSO links, across ≥4 randomly selected single subcarriers encompassing the entire tuning window. Furthermore, we achieved maximum transmission capacities of 192 Gb/s over back-to-back (BTB) configuration, and 168 and 176 Gb/s over 10 km SMF and 16 m indoor FSO channel, respectively, utilizing ∼1610 nm subcarrier, which are the record data rates reported in mid L-band subcarriers. Finally, for the first time to our knowledge, we demonstrate 128 Gb/s successful transmission over hybrid 11 km–8m–11 km fiber-FSO-fiber system employing ∼1608 nm subcarrier, thus strengthening the potential of this alternate network infrastructure in future optical access networks.

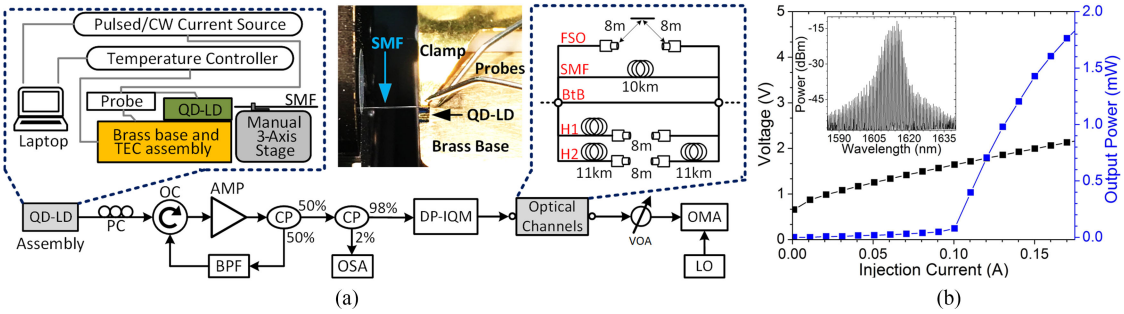


Fig. 1. (a) QD-LD self-injection locking and transmission experimental setup. The left, center and right insets show the probing assembly, zoomed view of a bare QD-LD butt coupled to a SMF and the various optical channel employed, respectively. (b) SMF coupled *L-I-V* characteristics of $3 \times 600\,\mu m^2$ QD-LD under CW operation. The inset shows the free running lasing spectrum at 110 mA biased current.

## 2. Tunable Self-Injection Locked QD-LD

We utilized a bare $3 \times 600\,\mu m^2$ ridge-waveguide L-band quantum dash-in-a-well laser diode whose growth and characterization under both pulsed current and continuous wave (CW) operations are available in [27]. The device was temperature controlled throughout the experiment at 14 °C using thermo-electric cooler module, as shown in the assembly of Fig. 1(a). The single facet output power of QD-LD was butt coupled into a lensed SMF via a 3-axis manual translation stage, and the free running lasing spectrum was observed on an optical spectrum analyzer (OSA) with 0.06 nm-bandwidth resolution. The *L-I-V* characteristics of $3 \times 600\,\mu m^2$ QD-LD under continuous wave (CW) operation is shown in Fig. 1(b) exhibiting a threshold current of 100 mA and maximum SMF coupled power of ∼1.9 mW (∼2.5 dBm) at 180 mA. The above threshold lasing spectrum of the QD-LD at a bias current of 110 mA, shown in the inset of Fig. 1(b), was found to have a total fiber coupled power of ∼0.4 mW (∼−4 dBm), with ∼5% (−13 dB) coupling efficiency. The broadband lasing emission is centered at ∼1615 nm with −3 dB-bandwidth of 7−10 nm and longitudinal mode spacing of 0.6 nm (70 GHz free spectral range).

The configuration of tunable self-injection locked QD-LD and the transmission setup is illustrated in Fig. 1(a). An L-band erbium doped fiber amplifier (EDFA) with a 20-dB gain and a TBPF (Santec OTF-350 flat-top filter shape, variable ∼0.1–15 nm bandwidth) with ∼7 dB insertion loss was connected to the bare QD-LD coupled SMF in a feedback loop via an optical circulator (OC). Besides, a polarization controller (PC) was directly applied to the QD-LD coupled SMF to maximize the locking efficiency [25]. It is noteworthy to mention that the TBPF allowed filtering out a selected single FP mode, to be re-injected into the QD-LD via OC and hence assisting in self-injection locking of that particular FP mode and achieving tuning. Next, a 3-dB coupler (CP) was employed between EDFA and TBPF to extract the locked mode from the feedback loop, for transmission experiments as well as monitoring (via another 2:98% coupler) purpose, as depicted in Fig. 1(a). In our configuration, EDFA served to compensate for the insertion losses of the TBPF and the SMF-laser coupling loss.

By tuning the central wavelength and passband of the TBPF in the feedback loop to match a selected FP mode, different individual QD-LD FP modes in the range ∼1602–1613 nm with 0.6 nm spacing were self-injection locked, as illustrated in Fig. 2(a). However, by mismatching the passband and the central wavelength of the TBPF with respect to the FP mode, injection locking disappeared and free running spectrum was recovered. Hence, the wavelength values of the modes, observed during QD-LD free running mode, should be well respected during the self-injection. Arbitrarily 9 different FP modes were self-injection locked from the available ∼18 modes, exhibiting ∼11 nm tunable window, as shown in Fig. 2(a) and (b), thus demonstrating the potential of our proposed broadly tunable self-injection locked QD-LD. It is worth mentioning that the FP mode spacing could be tailored to meet the coarse- or dense-WDM standards by proper selection of laser cavity length. moreover, Fig. 2(a) shows that only a small overlap is witnessed between the

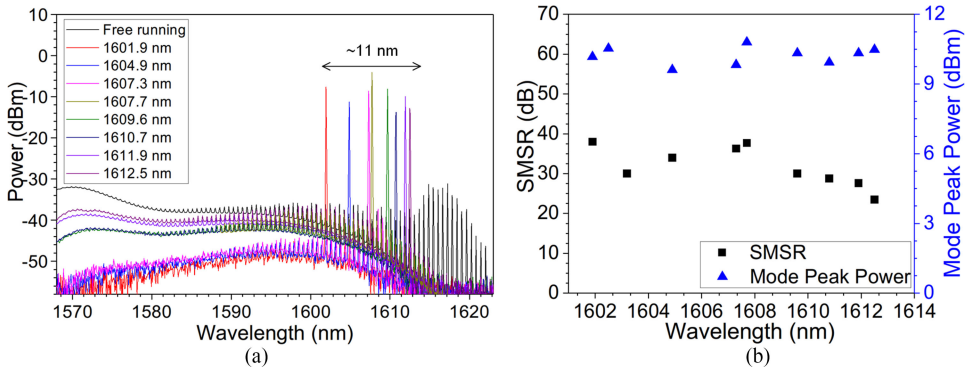


Fig. 2. (a) Free running lasing spectrum and self-injection locking of different FP modes (measured at 2% coupler output). (b) Integrated mode power (measured at 98% coupler output) and SMSR of the tunable self-injection locked QD-LD.

free-running emission spectrum of the QD-LD and the passband window of the EDFA. As a result, lasing FP modes lying outside this small overlap, which constitute the majority of the lasing bandwidth, could not be utilized as an injection-lockable mode, thus limiting the tunability. With that said, should a more compatible EDFA be acquired with an amplifying wavelength window that is more in line with the used QD-LD's free-running spectrum, this would enable a substantial enhancement in the tuning window of self-locked FP modes. We estimate the tunability to exceed double that of the current number of modes *i.e.*, $>$36 modes or $>$20 nm tuning window, in addition to large SMSR and mode power, and consequently achieving even higher data rates. Notice that the self-locked FP modes beyond $\sim$1612 caused considerable reduction in the SMSR ($<$25 dB), as summarized in Fig. 2(b). This is a direct consequence of operating EDFA outside its amplification window which substantially reduced the gain in that wavelength region with subsequent increase in the amplified spontaneous emission (ASE) near $\sim$1570 nm. This essentially elucidates the trend of the reduction in SMSR and mode power at longer wavelength self-locked FP modes compared to shorter wavelengths, thus exhibiting a flatness of $\sim$1 dB, while the SMSR was $>$28 dB up to $\sim$1612 nm. Furthermore, the utilized QD-LD was an un-optimized active region device with inferior L-I-V and spectral performance under CW operation. Employment of an optimized active region QD-LD would enable accomplishment of $>$50 nm wavelength tunability encompassing $>$90 FP modes since a -3dB bandwidth of $\sim$50 nm has already been reported in [26] under pulsed current operation. Besides, the self-locking arrangement could potentially be replaced by a customized single fiber Bragg Grating (FBG) with specific reflectivity and tunable wavelength, by exercising assisted piezoelectric and/or temperature control, for successful self-seeding. This would result in a cost-effective, energy efficient, compact and practical arrangement for commercial deployment.

Next, we systematically investigated the effect of locking behavior by comparing the short-term stability test of three different self-locked modes, 1603.2, 1609.6 and 1613.2 nm, covering the entire tunable band, over 20 min period, as shown in Fig. 3(a)–(c). Comparison across the figures indicated that the mode peak power and SMSR were more stable, within $\pm$0.1 dBm and $\pm$1 dB, respectively, for longer wavelength FP modes. In other words, locking was found to be more stable for the modes closer to the central lasing wavelength of the QD-LD, in spite of smaller peak power and SMSR. This is attributed to more appreciable contribution of coherent photons emitting near the QD-LD central lasing wavelength taking part in the locking process. In general, all the three FP mode wavelengths were also stable over the entire time period, thanks to the improvement of the QD-LD linewidth enhancement factor due to self-injection locking [27]. Lastly, we also identified the minimum injection ratio (*i.e.*, the feedback mode power to the free running mode power ratio, calculated at the QD-LD facet) required to sustain locking by increasing the mode peak power via varying the EDFA gain and observing the SMSR of 1609.6 nm FP mode, as shown in the inset

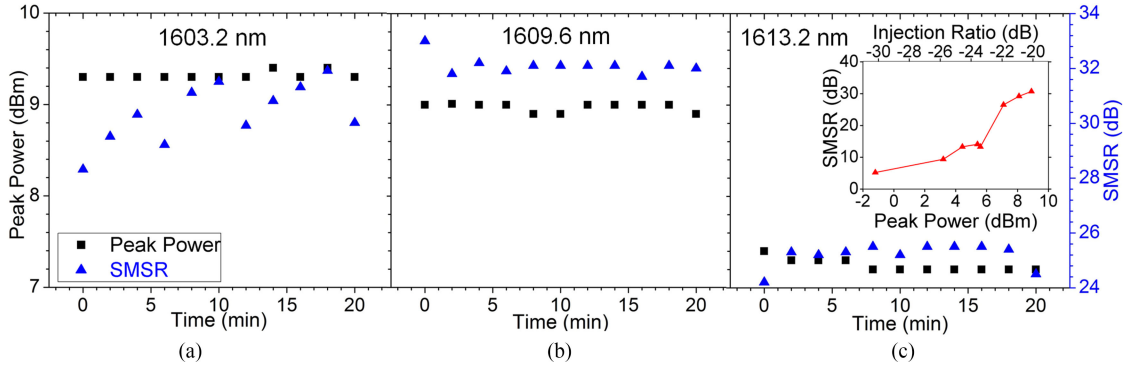


Fig. 3. Short-term stability test of the mode peak power and SMSR at (a) 1603.2, (b) 1609.6, and (c) 1613.2 nm self-locked FP modes. The inset of (c) depicts the effect of varying the 1609.6 nm locked mode peak power (or injection ratio) on the SMSR.

of Fig. 3(c). An abrupt increase in the SMSR from ∼11 to ∼26 dB was observed on increasing the mode power from ∼5.5 to ∼7dBm. Hence, this is the minimum mode power required to sustain locking, corresponding to ∼−22 dB injection ratio. Although the injection ratio was low, self-injection locking was sustained due to the feedback configuration that forced the filtered single FP mode to persist and amplify via the laser active region.

## 3. Tunable QD-LD in High Capacity Optical Communication

The data transmission setup is also shown in Fig. 1(a) where the selected self-locked FP mode, with mode power ∼9 dBm, was picked from the 98% end of the coupler and fed into the dual polarization in-phase quadrature (DP-IQ) external modulator. Pre-processing of the data signal was performed using MATLAB by generating pseudo random binary sequence (PRBS) with $2^{11}-1$ length, via an arbitrary wave generator (Keysight AWG M8195A), which is mapped into two levels electrical signal in order to obtain QPSK format; more details could be found in [24]. The data transmission was characterized under BTB, over 10 and 20 km SMF lengths, 16 m indoor FSO link, and hybrid 11 km SMF-8 m indoor FSO and 11 km SMF-8 m FSO-11 km SMF links, before being detected and analyzed by Keysight optical modulation analyzer (OMA-N4391A). A variable optical attenuator (Keysight VOA-N7764A) with ∼1 dB insertion loss was utilized before the OMA to study error-vector-magnitude bit-error-rate (BER) versus the received power. The indoor 16 m FSO link was built in the laboratory by 3-axis manual translation stage and implemented using two SMF collimators (Thorlabs F280APC) and a broadband mirror (Thorlabs BBT-E04). In the case of hybrid fiber-FSO system, an indoor 8 m FSO link is realized and tested in a similar manner as that of 16 m FSO link, as discussed above, except that the broadband mirror is excluded.

### *3.1 SMF Communication*

Fig. 4(a) shows the transmission results of DP-QPSK scheme at 25 Gbaud (100 Gb/s), over 20 km SMF, utilizing 8 separate subcarriers (self-locked modes) from ∼1602−1613 nm range. The measured BER was found to be below FEC limit ($3.8 \times 10^{-3}$) in all the cases at a stable average received power of ∼−11 dBm, after exhibiting 14 (7) dB modulator (TBPF) loss and fiber loss of 0.3 dB/km. The corresponding received clear constellation diagrams are shown in the insets of Fig. 4(a) and affirms possibility of ≥100 Gb/s/channel transmission across the tuning window. It is worthy to note that the measured BERs corresponding to ≥1612 nm locked modes in Fig. 4(a), are overestimated values and can be straightforwardly improved using additional filtering. In fact, the received power in both measurement cases includes non-negligible ASE background noise [over large spectral interval: ∼1570–1610 nm, see ASE levels in Fig. 2 (a)] that can be filtered using an appropriate L-band TBPF. Next, to test the data limit of these self-locked FP modes, a single

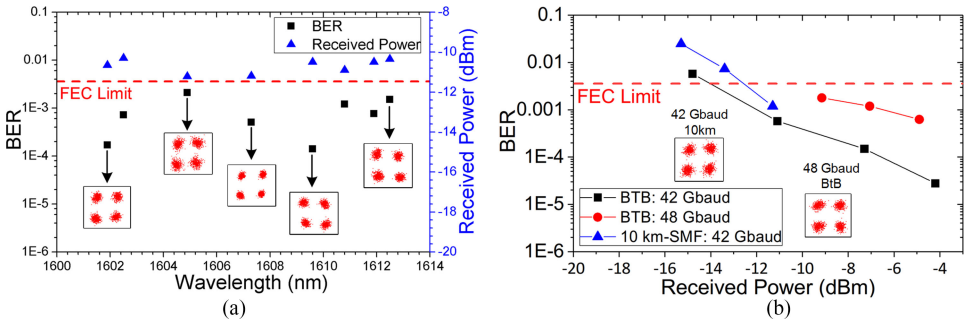


Fig. 4. (a) measured BERs after 20 km SMF transmission of 100 Gb/s DP-QPSK signal utilizing different self-locked modes of QD-LD, covering the entire ∼11 nm tuning window. (b) measured BERs versus the received power for the 1609.6 nm self-locked FP mode. The insets in (a) and (b) corresponds to the QPSK constellation diagrams.

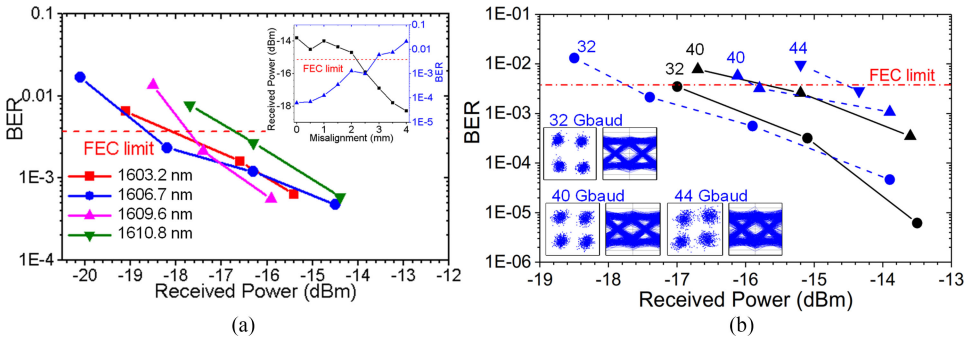


Fig. 5. (a) measured BER versus received power for 32 Gbaud DP-QPSK signal transmission over 16 m FSO link employing four different self-injection locked FP subcarriers as a source, from the available tuning range. Inset shows the effect of laser beam misalignment on the BER and received power for the 1609.6 nm subcarrier. (b) BER versus received power at different symbol rates for DP-QPSK transmission over BTB (black) and 16 m FSO channel (blue), at a fixed 1609.6 nm subcarrier. The insets show corresponding constellation and eye diagrams at a received power of ∼−14 dBm.

1609.6 nm mode was selected as a subcarrier to transmit DP-QPSK signal at different data rates, utilizing various channels. Successful transmissions of 168 Gb/s over 10 km SMF was achieved with a below FEC limit receiver sensitivity of ∼−12 dBm, as plotted in Fig. 4(b). While a power penalty of ∼1.6 dB was measured compared to the BTB configuration, clear constellation diagrams were obtained at a received power of −11 dBm, as shown in the inset of Fig. 4(b). Moreover, an effective transmission in the BTB configuration was also achieved at 192 Gb/s data rate with receiver sensitivity of ∼−9 dB, however, via 10 km SMF resulted in BER just above FEC limit. This data rate limitation is partly attributed to the larger linewidth (∼0.06 nm) of the self-locked FP modes which could further be improved by applying high reflection coating on QD-LD facets. Hence, these results, exhibiting ∼3 b/s/Hz spectral efficiency, demonstrate the feasibility of employing the proposed tunable mid L-band self-injection locked QD-LD as a promising source in next generation optical networks, in particular 100G NG-PONs.

### *3.2 Indoor FSO Communication*

For indoor FSO transmission, four different self-locked FP modes at ∼1602–1613 nm range with ∼9 dBm average mode peak power are selected as subcarriers for 32-Gbaud (128 Gb/s) DP-QPSK signal over 16 m FSO channel length. Fig. 5(a) plots the corresponding measured BER versus the received power, showing a receiver sensitivity of ∼−18 dBm for the first two subcarriers and ∼−17.5 and ∼−16.5 dBm for the latter ones, is required to maintain BER below the FEC limit. By comparing

the receiver sensitivities for both extreme modes, namely 1603.2 and 1610.8 nm, a power penalty of ∼2.5 dB suggests transmission performance degradation for the longer wavelength subcarriers. This is ascribed to a weaker injection ratio as a result of small mode power, which has been comprehensively discussed before. This shows the capability of the tunable self-locked QD-LD in attaining ≥128 Gb/s/channel transmission across the entire tuning window. Furthermore, in order to investigate the maximum possible transmission capacity of the tunable modes, 1609.6 nm single self-locked FP mode was again selected as a subcarrier and modulated with 32, 40 and 44 Gbaud (128, 160 and 176 Gb/s), and transmitted over BTB and 16 m indoor FSO channels. Fig. 5(b) summarizes the DP-QPSK transmission results for both channel configurations. As depicted, receiver sensitivities required to maintain an error-free transmission (*i.e.*, BER below FEC limit) were estimated to be ∼−17 (128), ∼−16 (160) and ∼−14.5 dBm (176 Gb/s). The former two cases exhibited ∼0 dB power penalty due to the FSO channel when compared to BTB configuration that might be due to negligible channel loss as a result of indoor environment. Hence, up to 176 Gb/s data rate with a spectral efficiency of ∼3 b/s/Hz is achievable over the indoor 16 m FSO link by the self-seeded L-band sub-carrier, thus highlighting the potential transmission capability of these self-seeded FP modes. Furthermore, the insets of Fig. 5(b) show the constellation and eye diagrams at a fixed received power of ∼−14 dBm for all the data rates. Open eyes and clear constellations further uphold the signature of error-free transmission.

Thereafter, in order to investigate the misalignment effect on the FSO link transmission performance, 1609.6 nm locked mode is utilized, and the reception collimator was gradually displaced with a radial step size of 0.5 mm while measuring the BER and the received power. The results are plotted in the inset of Fig. 5(a), showing a maximum misalignment tolerance of ∼2.8 mm with ∼17.5 dBm received power while maintaining a BER below the FEC limit. This corresponds to roughly a beam area misalignment of ∼60% at the receiver end (neglecting beam diffraction) [28]. A quasi-linear decrease of received power is observed with misalignment. In fact, the received power decreases by ∼2 dB for 3 mm misalignment. On the other front, the BER linearly (logarithmic) increases from $1.3 \times 10^{-4}$ up to $2.1 \times 10^{-2}$ when misalignment is increased from 1 to 4 mm. We also estimated an accessible emission limit (AEL) for eye safety by considering maximum attainable power at the onset of the FSO transmitter collimator (after modulation) as ∼−3 dBm. In this case, assuming the worst case ∼3.6 mm, which is equivalent to the diameter of the collimator's output beam, the optical power density is estimated to be 4.9 mW/cm$^2$ which is way below 100 mW/cm$^2$ according to the IEC 60825-1 standard limit for Class 1 classification for 100 m operations, thus qualifying our laser operation as safe under all conditions of normal use [28].

### *3.3 Hybrid Fiber-FSO Communication*

The previous discussions of fiber and FSO links has culminated into this part where a hybrid fiber-FSO system is implemented. This particular architecture is of a great significance to investigate as it emulates the scenario where two afar SMF networks are inter-connected via FSO links, for instance, racks within data centers, etc. [21]. As such, two configurations, depicted in Fig. 1(a), have been implemented, namely H1: 11 km SMF-8 m FSO, and H2: 11 km SMF-8 m FSO-11 km SMF employing a single locked 1607.7 nm subcarrier with ∼10.8 dBm mode power. Starting with channel H1, a successful transmission is achieved with a data rate of 32 Gbaud (128 Gb/s) in DP-QDPSK modulation scheme. As illustrated in Fig. 6, H1 channel exhibited a receiver sensitivity of -18 dBm for attainment of BER below the FEC compared to −18.5 dBm in BTB configuration with clear QPSK constellations. Thereafter, while adopting the same modulation scheme and data rate, the second hybrid channel was also investigated by inserting a second 11 km SMF at the receiver side. As shown in Fig. 6, a BER less than the FEC limit is achieved for received powers >−18 dBm, which is found to be comparable to the hybrid H1 counterpart. This is ascribed to the OMA post processing during demodulation by applying dispersion compensation algorithms. Moreover, this observation could also be a result of H1 and H2 channel measurements taken on different days which might have altered the locking efficiency (and mode power), thus affecting the receiver sensitivity. Nevertheless, clear constellation diagrams are achieved in this case thus

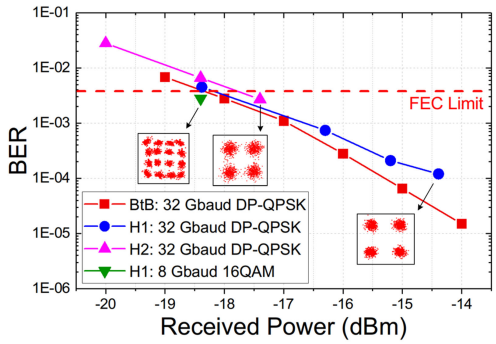


Fig. 6. Measured BER versus received power for 32 Gbaud (128 Gb/s) DP-QPSK and 8 Gbaud 16 QAM (32 Gb/s) signal transmission. While the former modulated scheme is investigated on both hybrid 11 km SMF- 8 m indoor FSO (H1) and 11 km SMF-8 m indoor FSO −11 km SMF (H2) channels, the latter one is investigated on only H1 link. In all the cases, 1607.7 nm self-injection locked FP mode is employed as a subcarrier. The insets show corresponding constellation diagrams at receiver sensitivities just below the FEC limit, and at ∼−14.5 dBm for the BTB configuration.

upholding error free transmission. Lastly, we conclude this work by reporting our initial results of employing higher order 16QAM modulation scheme over the hybrid channel H1. However, as a more sensitive modulation scheme with comparatively high power requirements, in addition to its associated higher insertion loss (*i.e.*, external modulator loss), successful transmission was attainable for 8 Gbaud symbol rate (32 Gb/s) with a below FEC limit BER of $2.6 \times 10^{-3}$ and a clear 16 QAM constellation diagram, as depicted in the inset of Fig. 6.

## 4. Conclusion

We investigated comprehensively the performance of tunable self-injection locked mid L-band QD-LD in terms of mode power and SMSR short-term stability analysis and injection ratio requirements, and demonstrated an extended tunability of ∼11 nm (∼1602–1613 nm). Promising results with stable >28 dB SMSR is achieved across the tuning window, thanks to the improved mode power and injection locking efficiency. Firstly, we successfully achieved 100 and 128 Gb/s DP-QPSK error-free transmission over 20 km SMF and 16 m indoor FSO channels utilizing various single self-locked modes across the tuning range. Besides, their potential to achieve >176 Gb/s transmission was demonstrated via successful DP-QPSK transmission of 192 Gb/s (BTB), 168 Gb/s (10 km SMF) and 176 Gb/s (16 m indoor FSO link) on ∼1610 nm sub carrier, thus exhibiting a potential aggregate capacity of >3Tb/s in mid L-band if all the tunable modes were to be used simultaneously in fiber/FSO based optical network. Furthermore, a successful 128 Gb/s data transmission was ultimately achieved over hybrid 11 km SMF-8m FSO-11 km SMF network in mid L-band region, thus strengthening the prospects of employing tunable L-band self-locked QD-LD as a source, and hybrid fiber-FSO as an alternate network architecture, in future WDM-PONs. This would enable cost-effective deployment of compact and unified transmitters with capability of mass production and deployment, to serve multi-subscribers, thus satisfying NG-PON source requirements.

## Acknowledgment

M. Z. M. Khan would like to thank Prof. B. S. Ooi and Dr. T. K. Ng from KAUST, as well as Prof. P. Bhattacharya and Dr. C-S. Lee from the University of Michigan.

## References

[1] Cisco, “Cisco visual networking index: Global mobile data traffic forecast update, 2016–2021,” White Paper Cisco, San Jose, CA, USA, 2017.

[2] D. Nesset, "PON roadmap [invited]," *J. Opt. Commun. Netw.*, vol. 9, no. 1, pp. A71–A76, 2017.
[3] J. I. Kani, "Enabling technologies for future scalable and flexible WDM-PON and WDM/TDM-PON systems," *IEEE J. Sel. Topics Quantum Electron.*, vol. 16, no. 5, pp. 1290–1297, Sep./Oct. 2010.
[4] M. A. Esmail, A. Ragheb, H. Fathallah, and M. S. Alouini, "Investigation and demonstration of high speed full-optical hybrid FSO/Fiber communication system under light sand storm condition," *IEEE Photon. J.*, vol. 9, no. 1, Feb. 2017, Art. no. 7900612.
[5] G. Parca, A. Shahpari, V. Carrozzo, G. Beleffi, and A. Teixeira, "Optical wireless transmission at 1.6-Tbit/s (16 × 100 Gbit/s) for next-generation convergent urban infrastructures," *Opt. Eng.*, vol. 52, no. 11, pp. 9772–9772, 2016.
[6] A. Sousa, A. Shahpari, V. Ribeiro, M. Lima, and A. Teixeira, "Gigabit passive optical networks and CATV over hybrid bidirectional free space optics +20 km single mode fiber," *Microw. Opt. Technol. Lett.*, vol. 57, no. 12, pp. 2867–2871, 2015.
[7] C. H. Yeh, C. W. Chow, Y. F. Wu, S. P. Huang, Y. L. Liu, and C. L. Pan, "Performance of long-reach passive access networks using injection-locked Fabry–Perot laser diodes with finite front-facet reflectivities," *J. Lightw. Technol.*, vol. 31, no. 12, pp. 1929–1934, Jun. 2013.
[8] M. C. Cheng, C. T. Tsai, Y. C. Chi, and G. R. Lin, "Direct QAM-OFDM encoding of an L-band master-to-slave injection-locked WRC-FPLD pair for 28 × 20 Gb/s DWDM-PON Transmission," *J. Lightw. Technol.*, vol. 32, no. 17, pp. 2981–2988, Sep. 2014.
[9] M. T. A. Khan *et al.*, "100 Gb/s single channel transmission using injection-locked 1621 nm quantum-dash laser," *IEEE Photon. Technol. Lett.*, vol. 29, no. 6, pp. 543–546, Mar. 2017.
[10] E. Wong, K. L. Lee, and T. B. Anderson, "Directly modulated self-seeding reflective semiconductor optical amplifiers as colorless transmitters in wavelength division multiplexed passive optical networks," *J. Lightw. Technol.*, vol. 25, no. 1, pp. 67–74, Jan. 2007.
[11] F. Y. Shih, C. H. Yeh, C. W. Chow, C. H. Wang, and S. Chi, "Utilization of self-injection Fabry–Perot laser diode for long-reach WDM-PON," *Opt. Fiber Technol.*, vol. 16, no. 1, pp. 46–49, 2010.
[12] S. Hann, D. Moon, Y. Chung, and C. S. Park, "Upstream signal transmission using a self-injection locked Fabry-Perot laser diode for WDM-PON," *Opt. Eng.*, vol. 44, no. 6, 2005, Art. no. 060509.
[13] T. Komljenovic, D. Babic, and Z. Sipus, "C and L band self-seeded WDM-PON links using injection locked Fabry-Pérot lasers and modulation averaging," in *Proc. OFC 2014*, 2014, pp. 1–3.
[14] M. Presi, A. Chiuchiarelli, R. Corsini, and E. Ciaramella, "Uncooled and polarization independent operation of self-seeded Fabry–Pérot lasers for WDM-PONs," *IEEE Photon. Technol. Lett.*, vol. 24, no. 17, pp. 1523–1526, Sep. 2012.
[15] J. N. Kemal *et al.*, "32QAM WDM transmission using a quantum-dash passively mode-locked laser with resonant feedback," in *Proc. OFC 2017*, 2017, pp. 1–3.
[16] M. A. Shemis *et al.*, "L-Band quantum-dash self-injection locked multiwavelength laser source for future WDM access networks," *IEEE Photon. J.*, vol. 9, no. 5, Oct. 2017, Art. no. 7905807.
[17] M. A. Shemis *et al.*, "Demonstration of L-band DP-QPSK transmission over FSO and fiber channels employing InAs/InP quantum-dash laser source," *Opt. Commun.*, vol. 410, pp. 680–684, 2018.
[18] H.-H. Lu *et al.*, "150 m/280 Gbps WDM/SDM FSO link based on OEO-based BLS and afocal telescopes," *Opt. Lett.*, vol. 41, no. 12, pp. 2835–2838, 2016.
[19] M. A. Esmail, A. Ragheb, H. Fathallah, and M. S. Alouini, "Experimental demonstration of outdoor 2.2 Tbps super-channel FSO transmission system," in *Proc. IEEE Int. Conf. Commun. Workshops*, 2016, pp. 169–174.
[20] Y. Yu, S. Liaw, H. Chou, H. Le-Minh, and Z. Ghassemlooy, "A hybrid optical fiber and FSO system for bidirectional communications used in bridges," *IEEE Photon. J.*, vol. 7, no. 6, Dec. 2015, Art. no. 7905509.
[21] A. S. Hamza, J. S. Deogun, and D. R. Alexander, "Wireless communication in data centers: A survey," *IEEE Commun. Surveys Tut.*, vol. 18, no. 3, pp. 1572–1595, third quarter 2016.
[22] S. A. N. Sousa *et al.*, "Real-time dual-polarization transmission based on hybrid optical wireless communications," *Opt. Fiber Technol.*, vol. 40, pp. 114–117, 2018.
[23] A. Shahpari *et al.*, "Ultra-high-capacity passive optical network systems with free-space optical communications," *Fiber Integrated Opt.*, vol. 33, no. 3, pp. 149–162, 2014.
[24] M. T. A. Khan, A. Ragheb, M. Esmail, H. Fathallah, S. Alshebeili, and M. Z. M. Khan, "4 m/100 Gb/s optical wireless communication based on far L–band injection locked quantum-dash laser," *IEEE Photon. J.*, vol. 9, no. 2, Apr. 2017, Art. no. 7901807.
[25] M. A. Shemis *et al.*, "Self-seeded quantum-dash laser based 5 m–128 Gb/s indoor free-space optical communication," *Chin. Opt. Lett.*, vol. 15, no. 10, 2017, Art. no. 100604.
[26] M. Z. M. Khan, T. K. Ng, C. S. Lee, P. Bhattacharya, and B. S. Ooi, "Investigation of chirped InAs/InGaAlAs/InP quantum dash lasers as broadband emitters," *IEEE J. Quantum Electron.*, vol. 50, no. 2, pp. 51–61, Feb. 2014.
[27] Q. T. Nguyen *et al.*, "16 × 2.5 Gbit/s downstream transmission in colorless WDM-PON based on injection-locked Fabry-Perot laser diode using a single quantum dash mode-locked Fabry-Perot laser as multi-wavelength seeding source," in *Proc. 2009 Conf. Opt. Fiber Commun.*, 2009, pp. 1–3.
[28] H. Kaushal, V. K. Jain, and S. Kar, *Free Space Optical Communication*. New York, NY, USA: Springer, 2017.